

# High Speed Interrogation of the Near-Field Plume of a 6-kW Laboratory Hall Thruster

IEPC-2009-112

*Presented at the 31st International Electric Propulsion Conference,  
University of Michigan • Ann Arbor, Michigan • USA  
September 20 – 24, 2009*

M.S. McDonald<sup>1</sup>, R.B. Lobbia<sup>2</sup> and A.D. Gallimore<sup>3</sup>  
*Plasmadynamics and Electric Propulsion Laboratory (PEPL)  
University of Michigan, Ann Arbor, MI 48109, USA*

**Abstract:** This paper presents preliminary findings from high speed (2 MHz) synchronous measurements of discharge current and ion current density from the far field to very near field of a Hall thruster plume. Recent work in this vein has applied statistical methods to create transfer functions between the thruster discharge current and spatially resolved plume plasma properties, permitting a time-resolved reconstruction of plume properties from temporally disparate probe measurements. However, whereas these previous attempts used a stationary Langmuir probe several thruster diameters downstream from a relatively low-power 600 W thruster, this paper describes the use of a fast reciprocating probe in ion saturation to interrogate the very near field of a nominal 6-kW thruster, operating derated to 2.4 kW, while minimizing discharge perturbations as much as possible. We find excellent correlation between probe ion current and the discharge current with increasing phase lags moving axially downstream. The mean discharge current increases by 5-10% while probing the very near field, though the normalized peak-to-peak-fluctuation magnitude is unaffected. By far the largest current density is observed in the cathode plume.

## Nomenclature

|     |                |
|-----|----------------|
| $A$ | = Probe area   |
| $l$ | = Probe length |
| $r$ | = Probe radius |

## I. Introduction

The near-field plume of a Hall thruster, defined variously as the region within one thruster radius, diameter, or other characteristic length of the thruster exit plane, forms the bridge for electrons between the cathode and the discharge channel. While within the channel wall conductivity and turbulent transport have both been posited as mechanisms for electron transport, in the plume, absent walls, turbulence is necessarily the dominant effect. Many of the nonintrusive optical techniques for observing fluctuations or instabilities in this region lack either temporal or spatial resolution, motivating the continued investigation into direct physical probing techniques to increase our understanding of the time-resolved behavior throughout the near field.

In this paper we use a Langmuir probe in ion saturation, effectively a nude Faraday probe, and a high-speed 2 MHz data acquisition system to explore this region directly, in anticipation of future work applying statistical techniques

<sup>1</sup> Doctoral pre-candidate, Department of Applied Physics, [msmcdon@umich.edu](mailto:msmcdon@umich.edu)

<sup>2</sup> Doctoral candidate, Department of Aerospace Engineering, [lobbia@umich.edu](mailto:lobbia@umich.edu)

<sup>3</sup> Arthur F. Thurnau Professor, Department of Aerospace Engineering; Director, Plasmadynamics and Electric Propulsion Laboratory, [alec.gallimore@umich.edu](mailto:alec.gallimore@umich.edu).

pioneered by Lobbia<sup>12</sup> to recover time-resolved plasma properties in this region. For now we present results indicating excellent noise cancellation in the probe signal, acceptably low perturbation of the discharge current outside of the extreme near field (<0.05 thruster radii), and good continuity of time-averaged ion current density across a wide axial and radial range.

## II. Experimental Apparatus and Setup

### A. Vacuum Chamber

The Large Vacuum Test Facility (LVTF) at the University of Michigan is a cylindrical, stainless steel clad chamber 9 meters (m) long and 6 m in diameter. The chamber is maintained at high vacuum by 7 CVI model TM-1200 cryopumps with an aggregate pumping capacity of 245000 L/s of xenon. Chamber pressure is monitored with a Varian UHV-24 nude gauge and is supplemented during thruster operation with a MKS 925C Pirani gauge operable down to  $10^{-5}$  Torr.

### B. Hall Thruster

The thruster used for the study presented in this paper (henceforth “the thruster”) is a 6-kW laboratory model Hall thruster developed jointly between the University of Michigan, the Jet Propulsion Laboratory and the Air Force Research Laboratory. The thruster has eight individual outer magnet poles and a hollow inner pole housing a center-mounted lanthanum hexaboride ( $\text{LaB}_6$ ) hollow cathode. The thruster design point is a 300 V discharge with an anode xenon mass flow rate of 20 mg/s, or approximately 20 A discharge current. This paper focuses on a 2.4 kW operating condition at 120 V and 20 mg/s anode xenon mass flow rate with a 25% cathode flow fraction (CFF). While the design point CFF is only 7%, increased CFF values up to 25% in this voltage range have been shown to increase a wide range of performance metrics,<sup>3</sup> making this an interesting condition for closer study.

### C. High Speed Axial Reciprocating Probe (HARP)

The probe was fired radially in towards thruster centerline at 66 axial positions ranging from 0.01 to 10 thruster radii (TR) downstream on the HARP, a custom-built high-speed motion table. The HARP is capable of peak accelerations of 6 g’s and velocities of 3 m/s.<sup>4</sup> For this experiment, the HARP was operated at 2 m/s, limiting the residence time of the probe in the direct line of sight of the discharge channel to less than 300 ms. The test matrix of axial firing positions is shown in Figure 2; the matrix consists of four successively finer overlapping grids concentrated near the thruster exit plane.

Previous studies<sup>4,5,6,7</sup> have used the HARP in an axial firing scheme to probe the interior of the discharge channel. The radial firing scheme used in this study eliminates the danger of an overshoot encountered in axial injection schemes, namely, the near-certain probe impact and destruction against the anode. While this precludes interrogation of the discharge channel itself, we are still able to approach within 0.01 thruster radii of the exit plane. Mounting the HARP vertically (see Figure 1) with its base secured to the chamber floor also has the salutary effect of minimizing the violent recoil of the stage during peak accelerations, which in turn reduces probe vibration and misalignment during firing.

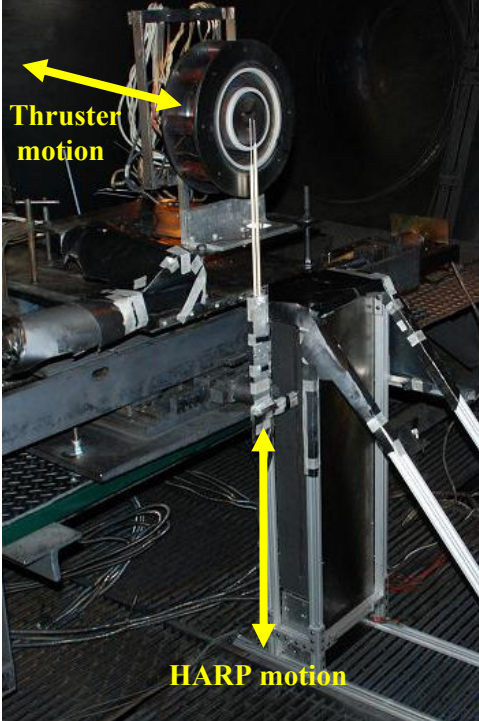


**Figure 1: HARP firing setup.** The HARP fires vertically (radially inward) from a fixed position while the thruster approaches axially on a motion stage.

| Grid       | Axial Span (Thruster Radii) | Resolution (Thruster Radii) |
|------------|-----------------------------|-----------------------------|
| Coarse     | 10.00                       | 0.25                        |
| Medium     | 1.25                        | 0.06                        |
| Fine       | 0.25                        | 0.03                        |
| Ultra-Fine | 0.06                        | 0.01                        |

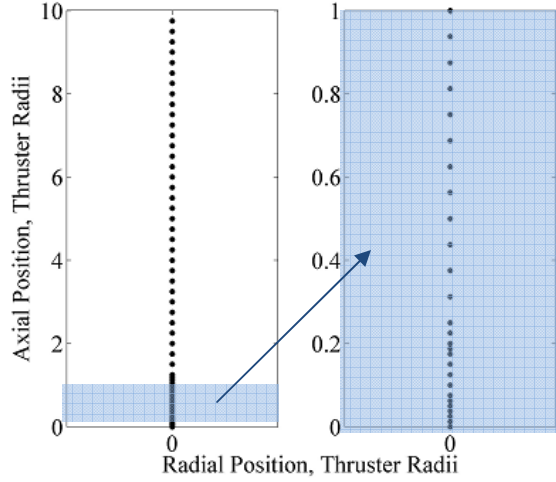


**Figure 2: HARP firing test matrix.** Each dot denotes a firing position. Four successively finer grids overlap, concentrating near the exit plane as seen in the closeup at right.

## D. Langmuir / Faraday probe

### 1. Operation in Ion Saturation

The probe used in this study was initially conceived of as a high-speed ( $\sim 50$  kHz) swept Langmuir probe, following in the footsteps of previous work<sup>1,2</sup> on a cluster of low-power BHT-600 Hall thrusters. In those experiments it was possible to eliminate the stray capacitance in the probe circuit to an extraordinary degree through the use of low-capacitance signal wire, careful suspension of the signal wire away from ground planes in the vacuum chamber, and the use of an insulated null probe paired with an active Langmuir probe in a double-bore alumina probe body.

In this work, we follow these steps as far as possible, using the same low-capacitance wire and null probe technique. However, with the use of the HARP it was not possible to reproduce the same level of ground plane isolation as previously achieved. The HARP is encased in a stainless steel shroud to shield the motor hardware from undue plasma bombardment and heating, and in order to reach the probe tip the signal wires must pass into and out of this shroud. Once inside the shroud, they also pass through a flexible cable guide that they share with the HARP power cabling.

Possibly due to this poor ground plane isolation, we were unable to confidently correct for the leakage current induced at high sweep speeds, and instead operated the Langmuir probe effectively as a Faraday probe at a fixed -24 V, solidly in ion saturation. Lacking a full voltage sweep for the probe, it is difficult to extract meaningful ion densities from the probe current signal. However, considering the probe as a nude Faraday probe offers another avenue, to interpret the probe current as proportional to the local ion current density. Additionally, we are able to observe these current density fluctuations 20 times faster than we could observe the ion density by sweeping at 50 kHz.

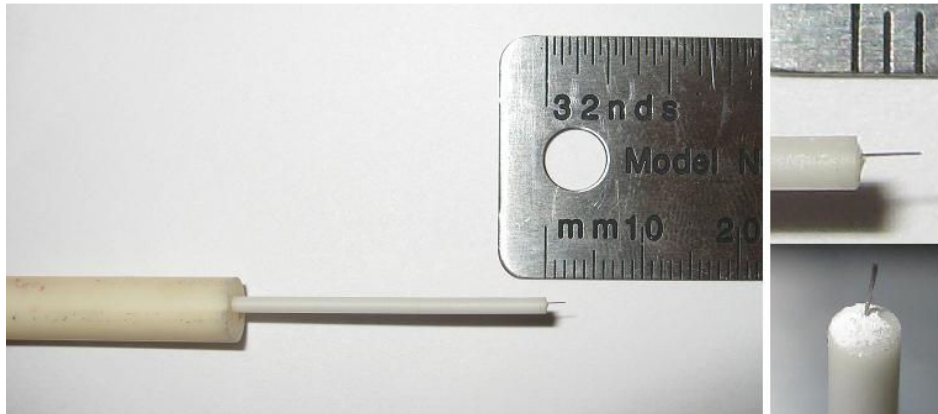


**Figure 3: Langmuir probe tip, with close-ups.** Clockwise from left: the telescoping alumina rods that support the probe electrode; a closeup of the probe tip, approximately 2 mm in length; and a top view of the probe tip, showing the Ceramabond sealant capping off the null probe.

The use of the probe in ion saturation only, coupled with the small size of the probe, led to probe current signals less than one milliamp even in the very near field; nevertheless, it was still possible to clearly discern the behavior of these signals above the electrical noise.

## 2. Probe Construction

The probe electrode is made of tungsten wire 0.13 mm (0.005") in diameter, encased in a 61 cm (24") double-bore alumina rod 1.6 mm (0.0625") in diameter. The thin double-bore alumina rod is in turn encased in another, larger double-bore alumina rod, slightly shorter than the first and 6.4mm (0.25") in diameter. The double-bore of the larger rod allows for a snug fit of the smaller rod and reinforces it during firing. The outer alumina rod is in turn encased by a 30 cm (12") stainless steel tube sized to tightly accommodate the large alumina rod. This stainless shell provides a durable surface to clamp securely onto without fracturing the brittle alumina.

The length of the probe permits retraction to a home position safely outside the main body of the plume after firing, while the narrow body minimizes the exposed surface area in front of the discharge channel and cathode during firing.

The exposed probe tip is approximately 2 mm long, and the cap of the alumina rod is sealed off with Ceramabond, fully insulating an unexposed "null" probe in the other bore. This null probe aids in correcting the signal from the active probe for stray capacitance effects during voltage sweeps, or from electrical noise in general.

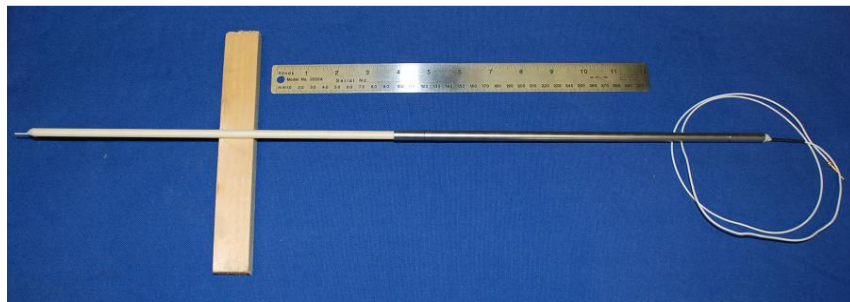


**Figure 4: Langmuir probe for use with HARP and probe rake.** The probe body is over two feet long but only a quarter inch in diameter.

The probe is still relatively fragile and unwieldy, and care must be taken to attach and align it to the HARP carriage to avoid lateral vibrations from the high accelerations seen during firing. A mechanism designed for this purpose, dubbed the "probe rake" because it can support up to four probes at once in a raking action across the plume, is shown in Figure 5. An early cantilevered design for the probe rake, still visible in Figure 1, suffered substantial lateral vibrations due to beam flexing during acceleration, and was discarded in favor of the in-line design of Figure 5. The rake attaches directly atop the HARP carriage, such that the probe axis and acceleration axis are very nearly collinear.

The probe is secured into the probe rake with three set screws spaced 10 cm (4"). We use screws with tapped heads and run lock wire through them such that each screw secures its neighbors, lest the repeated jarring of the HARP acceleration during firing work the set screws loose,. Finally, once the probe is secured to the rake, the upstream face of the rake is shielded in Grafoil and secured to the HARP carriage.



**Figure 5: Probe rake.** The probe rake secures the probe body with three set screws, which are in turn fastened in place by lock wire. The rake attaches directly to the HARP carriage through holes in the two cross-beams at right.

#### E. Data Acquisition

The entire data acquisition process is automated through LabView programs running on two PCs, one controlling thruster axial motion and HARP firing and the other dedicated to data acquisition. Upon arrival at each test grid point the motion PC triggers the HARP to fire and the data PC to begin acquisition. The data PC houses an 8-channel 16-bit analog input board capable of simultaneous sampling at 2 MHz via independent digital-to-analog converters for each channel. A complete sweep of the test grid described in this paper takes about 15 minutes, with 10-15 seconds between each firing.

At each point the data PC acquires voltage signals from the active and null probes, the HARP position encoder, and an F.W. Bell NT-50 magnetoresistive sensor monitoring the discharge current.

### III. Results

#### A. Null Probe Noise Reduction

Figure 6 shows the probe signal profiles from a firing near the thruster exit plane. The hump in the active current near 100 ms is due to the discharge channel, as indicated by the probe position passing through  $r = 1$  thruster radius. Both the active and null probes exhibit substantial noise levels, but the corrected probe current,

$$\text{Corrected Current} = \text{Active Current} - \text{Null Current} \quad (1)$$

is visibly improved over both raw probe signals, from about 0.05 mA to less than 0.01 mA. While in the near-field the null correction clarifies an already self-evident signal, in the far field the signal amplitudes themselves are of this order ~0.01 mA and the null probe correction makes it possible to identify an otherwise invisible signal.

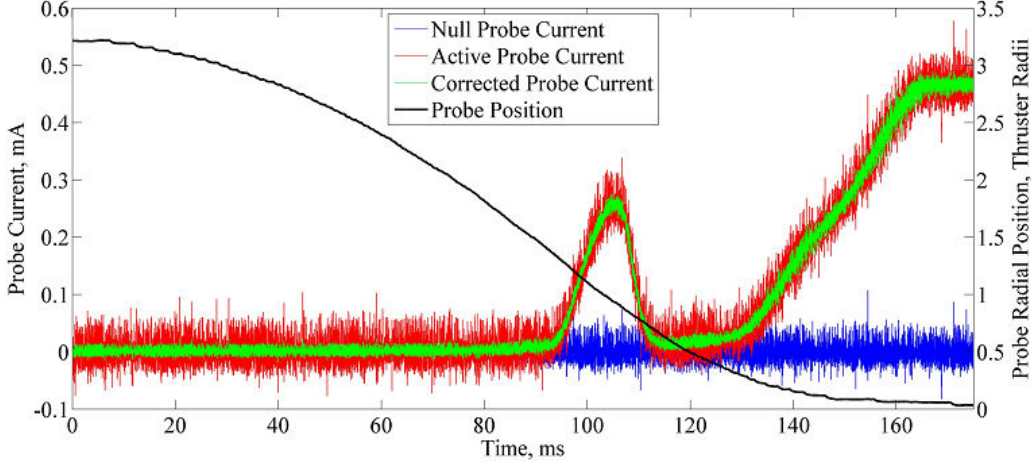


**Figure 6: Snapshot of a HARP firing near the exit plane.** The active probe signal jumps as the probe passes through the discharge channel ( $r = 1$  thruster radius), then peaks as the probe passes into the cathode plume near  $r = 0$ . The null signal substantially improves the signal quality by correcting for electrical noise independent of plasma fluctuations.

### B. Discharge Current / Probe Current Correlation

There is a visible correlation shown in Figure 8 between the corrected probe current and the discharge current signal. Such a correlation has been observed before and convincingly attributed to the well-known breathing-mode oscillation.<sup>1</sup> This interpretation is supported by the comparable magnitudes of the normalized fluctuations and by the increasing phase lag between the signals at downstream axial locations, consistent with a travel time delay of ions through the plume from the ionization region. Both signals exhibit strong power spectrum peaks (see Figure 7) in the 5 kHz range. Such oscillations are not generally noticeable at the nominal 300 V discharge voltage for this thruster; in fact, nominal operation is quite quiescent. However, at voltages of less than 150 V they become increasingly prevalent, and in several 120 V discharges at varying anode flowrates and cathode flow fractions they were quite common.

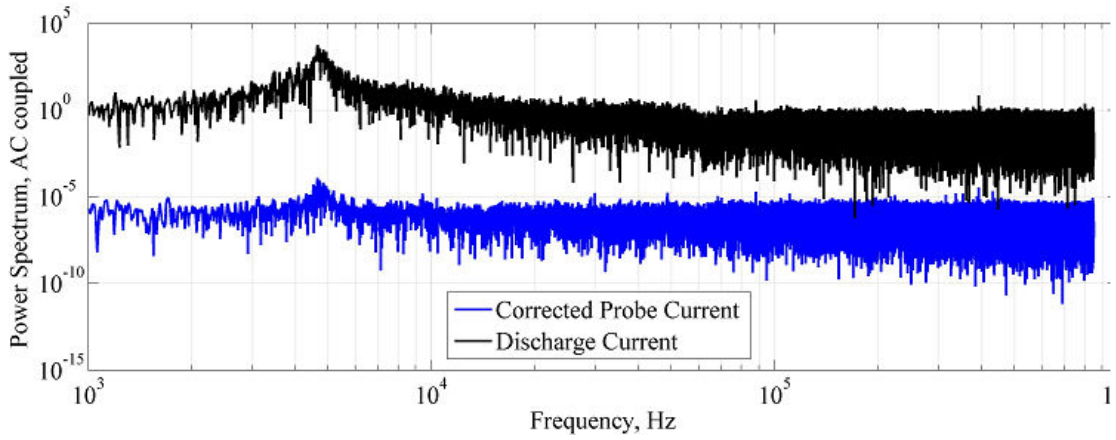


**Figure 7: Probe and discharge current power spectrum.** Both show noticeable peaks near 5 kHz. Since the probe current is roughly six orders of magnitude less than the discharge current, the power spectrum is as well.

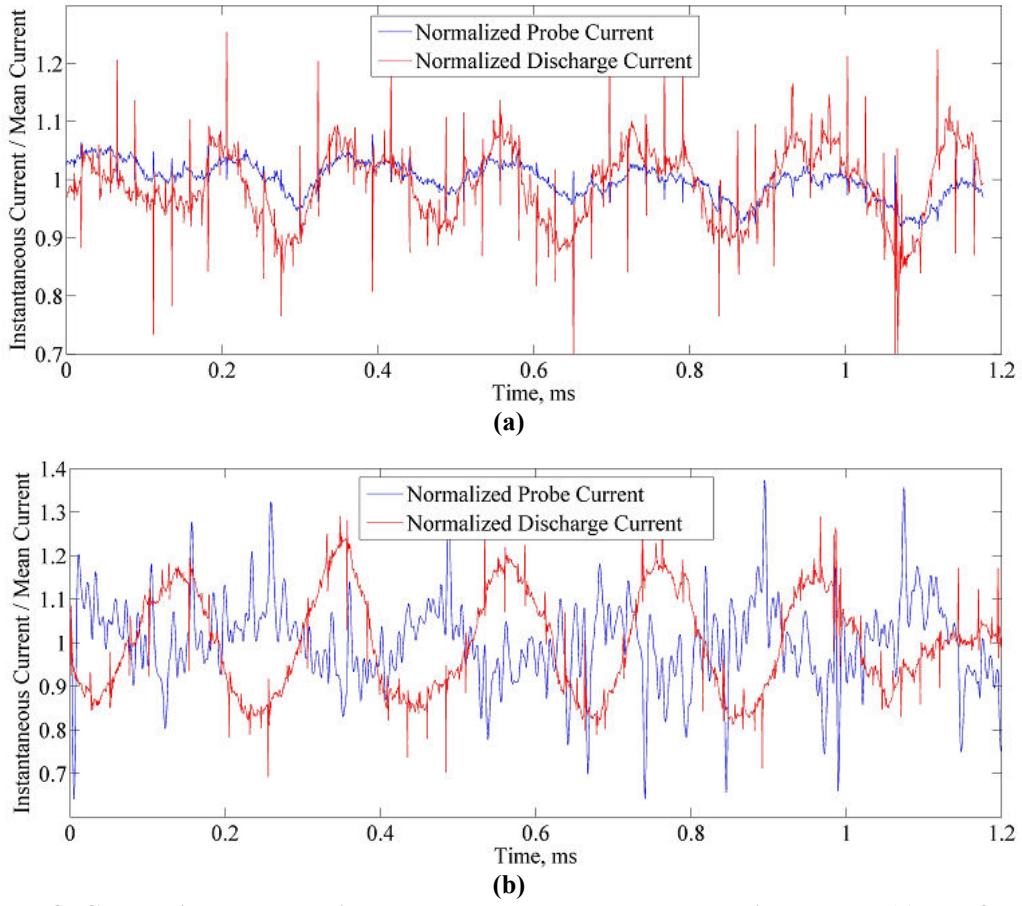


**Figure 8: Correlation between discharge current and probe current in the near (a) and far (b) fields.** In (a) the signals have a near-zero phase lag, while in (b) the signals are nearly opposite in phase.

Note that, while the sinusoidal breathing mode oscillation is quite evident in the samples shown above, it would be misleading to imply that the entire sample of the discharge current at any condition followed such a clean pattern. In general, the sinusoidal behavior above appears and disappears in cycles lasting several milliseconds; we have chosen the above examples for their visual clarity in illustrating this trend.

### C. Discharge Current Perturbation by Probe

One of the primary reasons for using the HARP was to minimize perturbations to the thruster discharge as much as possible. A common rule of thumb for evaluating such perturbations is to consider the discharge perturbed if the magnitude of fluctuations normalized to the mean discharge current exceeds 20%.<sup>4,7</sup> Figure 9 shows the discharge current signal as the HARP injects the probe into the plume near the exit plane; in the top half of the figure, the discharge current is shown with a moving average superimposed. This thin red line clearly shows a sudden increase in the mean value of the discharge current as the probe passes into the body of the plume, where  $r < 1$  thruster radius. However, Refs. [4,7] make little mention of the mean discharge as a figure of merit, and the bottom half of Figure 9 shows no increase in the normalized current for  $r < 1$ .

The probe clearly has an effect, as the mean discharge current changes by nearly 10%, but it is interesting that the normalized fluctuation magnitude is completely unchanged. Rather than inducing greater instability in the plasma, the probe ignores the transients, affecting only the DC behavior. Assuming a 10% increase in ion current due to increased ionization efficiency during probe insertion to be grossly unlikely, the probe body probably offers a radial bridge to the anode for electrons across the strong magnetic fields in the near-field plume.

Even this disturbance quickly dies out as the probe moves axially downstream. Figure 10 can be thought of as a stitching together of the local mean discharge current (in red) of Figure 9 for all axial firing locations. Noticeable

effects on the mean discharge current are visible only within the first half-thruster radius, and the dropoff from the 10% increase in the mean seen in Figure 9 occurs very rapidly.

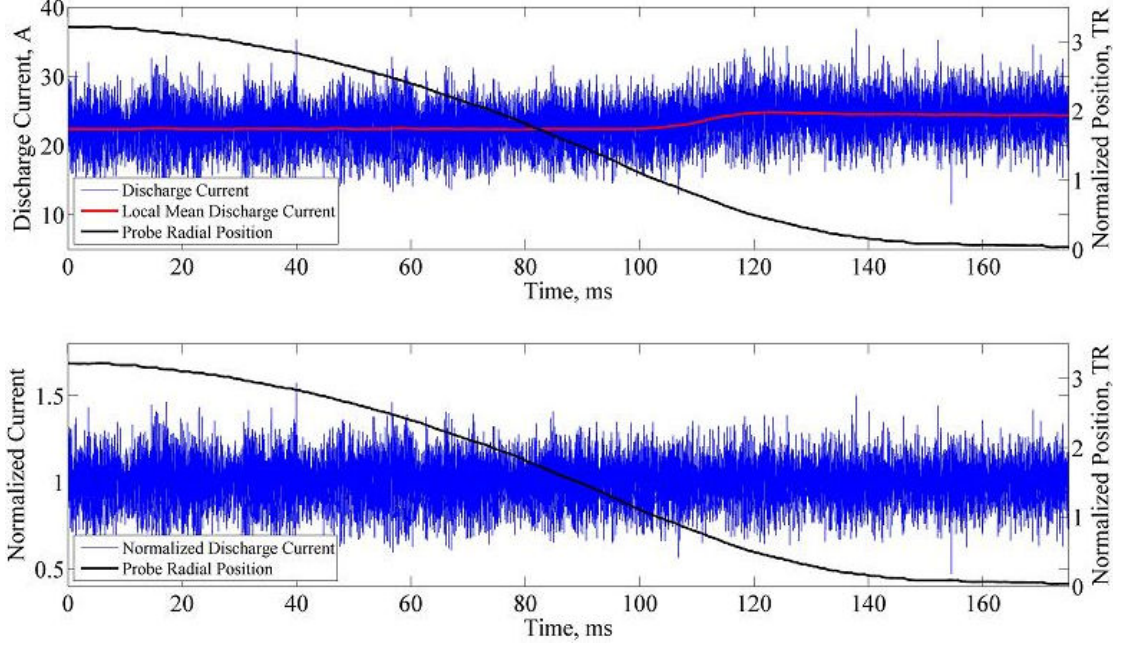


**Figure 9: Discharge current profiles in the near field, absolute (top) and normalized to local mean (bottom).** The increase in the mean discharge current is clear above, but the absence of any effect on the relative fluctuation level below is unexpected.

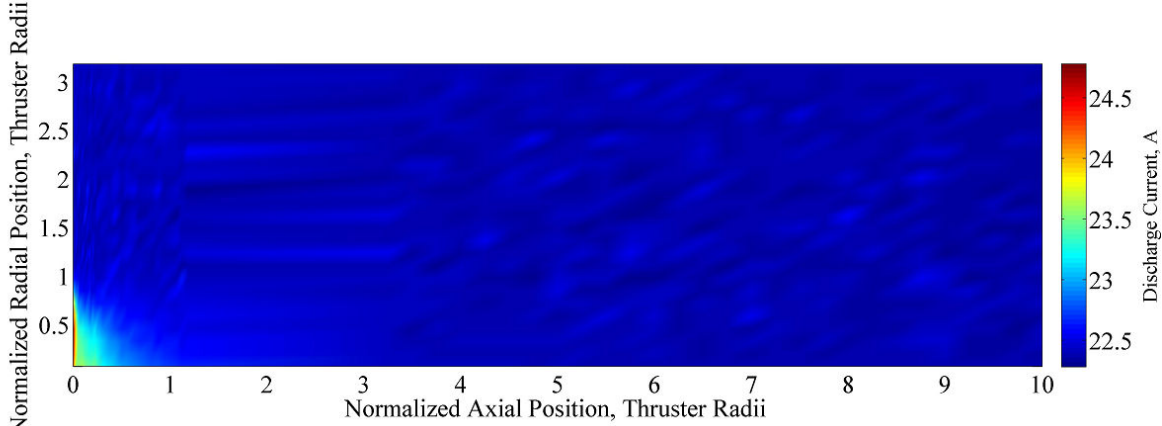


**Figure 10: Mean (time-averaged) discharge current across the full test grid.** Similar to the top half of the previous figure, this plot shows the full axial and radial breakdown of the discharge current response to the probe insertion. The probe has the most severe effect in the very near field in front of the cathode plume.

#### D. 2D Time-averaged Probe Current

Similar to Figure 10, Figure 11 stitches together the corrected probe signals (the green lines of Figure 6) over all the axial HARP firings to create a complete 2D map of the probe current. The brilliant spike of ion current from the cathode is dominant, washing out the less vivid spike at the discharge channel exit near  $r = 1$ . There is also a saddle point linking the discharge channel and cathode plumes, visible almost on the diagonal between the discharge channel exit and  $z = 1$  thruster radius on the thruster centerline. Finally, taking a naïve view (neglecting any sheath effects, for instance) of the probe tip as a nude Faraday probe with effective area  $A$  normal to the discharge of

$$A = 2lr = 2(2\text{cm})(.0064\text{cm}) \approx .0025\text{cm}^2 \quad (2)$$

then the units of probe current in Figure 11 may be converted to current density in the more familiar  $\text{mA}/\text{cm}^2$  by multiplying by a factor of  $1/A$  or approximately 400.

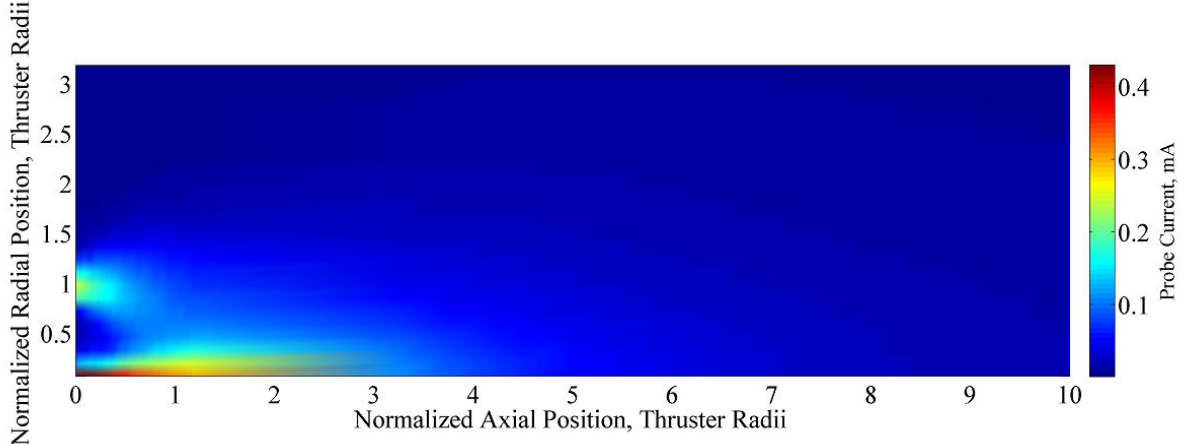


**Figure 11: Mean (time-averaged) probe ion saturation current across the full test grid.** Note the peak values near the orifice of the cathode, the saddle point linking the discharge channel and cathode plumes, and the slight pinch radially inward of the plume from the discharge channel.

#### IV. Conclusions

The salient features of this study are the high speed of probe insertion into the near field plume, the rapid sampling rate of the data acquisition system, and the minimization of discharge current perturbation due to the small probe size and operation in ion saturation. As a result, we are able to interrogate deeply into the near field before discharge current perturbations become noticeable and a cause for concern.

A null probe has proven extremely effective at increasing the signal to noise ratio of the probe, purely on the basis of electrical noise correction, without any stray capacitance to consider. The ease of implementing this technique, requiring as it does only a single extra data acquisition channel if implemented carefully, combined with the impressive results with a minimum of post-processing effort (direct subtraction was used in this paper), suggests that it be strongly considered during future Langmuir probe experiments.

Finally, a strong correlation between the power spectrum of the discharge current and probe saturation currents is observed, and a clear breathing mode oscillation is present in this low-voltage operation. Future work includes using the wealth of time-resolved data acquired in this study to statistically reconstruct the temporal evolution of the plume from a discharge current input signal (a la Ref. [1]); these observations bode well for that effort. Future work will also reexamine the viability of an axial injection scheme, possibly with an updated HARP system capable of higher speed and greater positioning fidelity, to determine which method is preferable for interrogating the near field. Discharge channel interrogation will, of course, still proceed via axial injection.

#### Acknowledgments

The first author would like to gratefully acknowledge the support of the National Science Foundation Graduate Research Fellowship Program and the Tau Beta Pi Foundation during his graduate studies. The authors would also like to acknowledge and thank the Air Force Office of Scientific Research for funding this work through grant FA9550-06-1-0105, under Program Manager Dr. Mitat Birkan. Finally, the first author would like to thank summer intern Logan Oonk, without whose assistance a summer of experimentation on an injured knee would have been impossible, and to offer his everlasting apologies for those occasions when, heading out to turn on the cryopumps, we were unhappily greeted by the dawn. *Mea culpa, mea culpa, mea maxima culpa.*

## References

- 
- <sup>1</sup> Lobbia, R.B. and Gallimore, A.D., *AIAA Joint Propulsion Conference*, “A Method of Measuring Transient Plume Properties,” AIAA-2008-4650.
- <sup>2</sup> Lobbia, R.B. and Gallimore, A.D., *AIAA Joint Propulsion Conference*, “Temporally and Spatially Resolved Measurements in the Plume of Clustered Hall Thrusters,” AIAA-2009-5354.
- <sup>3</sup> Brown, D.L., “Investigation of Low Discharge Voltage Hall Thruster Characteristics and Evaluation of Loss Mechanisms,” Ph.D. Dissertation, Department of Aerospace Engineering, Univ. of Michigan, Ann Arbor, MI 2009.
- <sup>4</sup> Haas, J.M., “Low-Perturbation Interrogation of the Internal and Near-Field Plasma Structure of a Hall Thruster Using a High-Speed Probe Positioning System,” Ph.D. Dissertation, Univ. of Michigan, Ann Arbor, MI 2001.
- <sup>5</sup> Reid, B.M. and Gallimore, A.D., *AIAA Joint Propulsion Conference*, “Langmuir Probe Measurements in the Discharge Channel of a 6-kW Hall Thruster,” AIAA-2008-4920.
- <sup>6</sup> Reid, B.M. and Gallimore, A.D., *AIAA Joint Propulsion Conference*, “Plasma Potential Measurements in the Discharge Channel of a 6-kW Hall Thruster,” AIAA-2008-5185.
- <sup>7</sup> Linnell, J.A., “An Evaluation of Krypton Propellant in Hall Thrusters,” Ph.D. Dissertation, Univ. of Michigan, Ann Arbor, MI, 2007.